11th International Symposium on Magnetic Bearings
August 26-29, Nara, Japan

A MAGNETICALLY LEVITATED BLOOD PUMP USING LCR CIRCUITS

H. Ming Chen, Peter A. Chapman, Arthur C. Donahue, Charles J. Prisco, and Thomas J. Walter
Foster-Miller, Inc., Albany, NY, USA 12205
mchen@foster-miller.com

ABSTRACT
An implantable blood pump has been developed for use as a left ventricular assist device (LVAD). The pump features total magnetic levitation of the shrouded centrifugal impeller. Sensorless levitation is achieved by using three ac magnets with tuned LCR circuits in the axial direction and a pair of permanent magnet rings in the radial direction. This paper describes design issues related to the pump's magnetic levitation system; pump impact on patient physiology is not addressed.

INTRODUCTION
The desire to make magnetic levitation (maglev) totally passive prompted this concept to apply a tuned LCR circuit technique to blood pumps. The LCR circuit is a self-sensing and self-positioning maglev technique [1, 2] with an electromagnet (L) connected in series with a capacitor (C) and a resistor (R) (Figure 1a). The LCR circuit is excited by a sinusoidal voltage source at a fixed frequency that is slightly above the circuit's resonant frequency. As the rotor moves away from the LCR, the gap on the LCR side increases and the inductance decreases. As a result, the circuit resonant frequency increases or becomes closer to the excitation frequency. Therefore, more ac current will be generated and thus more force to pull the rotor back towards the center or neutral position. If the gap decreases, the opposite is true. This mechanism is illustrated in the force-versus-gap plot of Figure 1b. The resistance (R) is a very important parameter that dictates the suspension force gradient with respect to the gap change or the stiffness.

Since the LCR magnetic suspension has no damping of its own, the damping required for dynamic stability comes from the pump rotor submerged in blood. For dynamic stability, the required damping may come from liquid [2], such as in the case of a pump impeller submerged in blood [3]. In a hybrid bearing application [4], which involves load sharing between a foil thrust bearing and an LCR magnetic bearing, the required damping was provided by the foil bearing.

It is possible to recreate displacement information from the current signal in the LCR circuit and use it to generate active damping. The recreated signal is fed back to modulate the excitation voltage and achieve damping [5]. However, like many sensorless schemes, this boot-strap method is difficult to implement. Applying squeeze-film liquid damping is therefore a preferable means to retain the control simplicity of the sensorless maglev technique.

Over several years and under grants from the National Institutes of Health (HL065819 and HL072610), we have developed this inherently controlled LCR circuit for use in an implantable left ventricular assist device (LVAD) [3, 6]. Shown in Figure 2, the pump consists of a one-sided permanent-magnet (PM) brushless dc axial-gap motor; a pair of axially polarized PM rings for radial support of the pump impeller (two radial degrees of freedom); and three independent, identically tuned LCR circuits, spaced evenly around the circumference for axial suspension, which provide control for three degrees of freedom, i.e., one axial translation and two rotations. Two of these pumps are operating on endurance test and have accumulated more than 13,000 operating hours at the design point of 5 liter/min and 100 mmHg.

DESIGN AND ANALYSIS OF A MAGLEV BLOOD PUMP USING LCR BEARINGS
One may imagine a model where the pump impeller is suspended horizontally. Connected to the impeller top are three LCR bearings like three springs, which are 120° apart and fixed to the bearing stator above. Also on the same side is a pair of magnet rings: one fixed on the impeller surface and the other fixed on the bearing stator. Serving as the radial bearing, the magnets have an attractive force that pulls the impeller up. Below the impeller is the axial gap motor, which exerts a magnetic force and pulls the impeller down.

Relevant Design Parameters
To achieve magnetic levitation of the impeller, the parameters that affect the rotor dynamics and static force balance must be considered:

- Axial pull (F_{lcr}) and axial stiffness (K_{lcr}) of each LCR circuit
- Angular stiffness created by the three LCR circuits ($K_{\theta lcr}$)

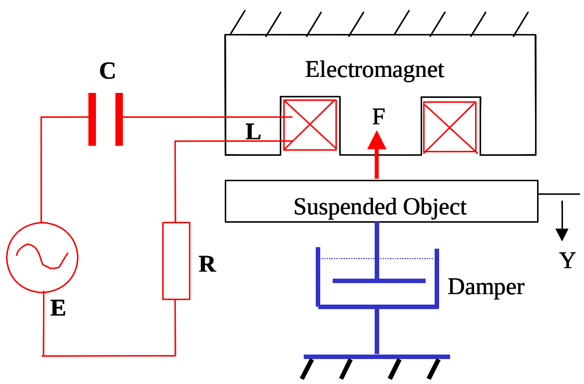

FIGURE 1a: LCR circuit

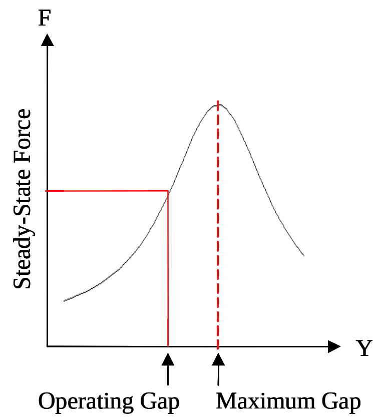

FIGURE 1b: Force versus gap plot

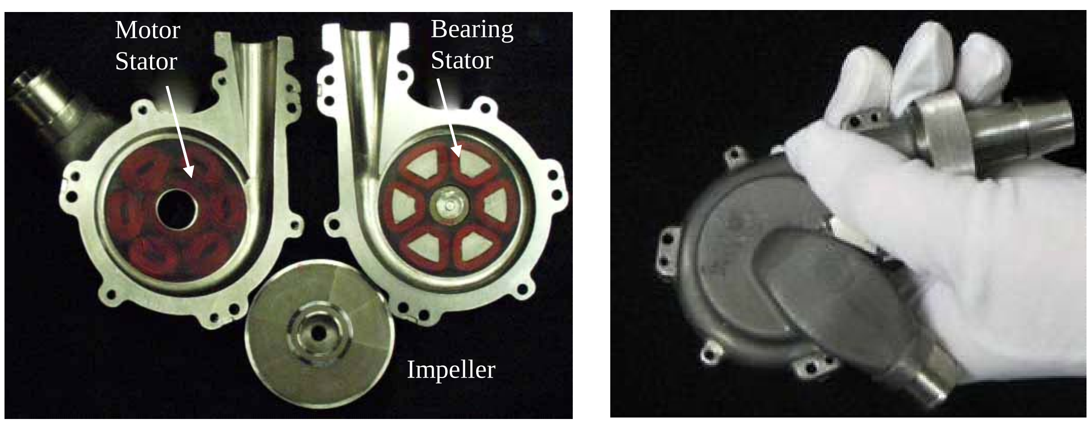

FIGURE 2: Implantable pump with inherently controlled LCR circuits

- PM bearing radial stiffness (K_{rpmb}), axial stiffness (K_{apmb}, a negative value), axial pull (F_{pmb}), and angular stiffness ($K_{\theta pmb}$, also a negative value)
- Motor axial pull (F_{motor}), axial stiffness (K_{amotor}, a negative value), and angular stiffness ($K_{\theta motor}$, a negative value).
- Impeller mass (M), transverse mass moment of inertia (I_t), and polar mass moment of inertia (I_p).

For a workable combination, the sum of the axial pulls must balance the impeller weight, that is,

$$3\,F_{lcr} + F_{pmb} - F_{motor} \pm Mg = 0 \qquad (1)$$

where g = gravity acceleration. The sign before "M" depends on the orientation of the pump assembly (i.e., motor side up or down, the two extreme positions for weight).

The sum of the axial stiffnesses must be positive, that is,

$$\Sigma K_a = 3K_{lcr} + K_{apmb} + K_{amotor} > 0 \qquad (2)$$

where $K_{apmb} = -2K_{rpmb}$ for the PM radial bearing with no nearby magnetic material.

The sum of the angular stiffnesses must be positive, that is,

$$\Sigma K_\theta = K_{\theta lcr} + K_{\theta pmb} + K_{\theta motor} > 0 \qquad (3)$$

where $K_{\theta lcr} = 1.5K_{lcr}\,R^2$ and R = force center radius of each tuned LCR. Also $K_{\theta pmb} = -2K_{rpmb}\,r^2$ and r = mean radius of PM bearing. It is readily derived that the motor angular stiffness is $K_{\theta motor} = K_{amotor}(R_o^2+R_i^2)/4$ for an outer radius R_o and an inner radius R_i.

The impeller radial, axial, and angular critical speeds depend on, respectively, the radial bearing stiffness (K_{rpmb}), the net axial stiffness (ΣK_a), and the net angular stiffness (ΣK_θ). For smooth operation, it is important to keep all critical speeds well damped or outside of the pump's operating speed range.

DYNAMIC ROTOR STABILITY SIMULATION

A time-transient dynamic simulation was performed with MATLAB to assess the dynamic rotor stability. The mathematical model (Figure 3) included the three degrees of freedom of the impeller, i.e., Z, θ_x and θ_y, and the three LCR circuits. The corresponding equations of motion are presented in Table 1.

The two uncoupled, lateral degrees of freedom (X and Y) and the impeller spin were excluded for simplicity. There were six second-order differential equations in the model including gyroscopic effects, which were integrated in time using the Runge-Kutta method with given initial conditions.

The PM radial bearing and the motor contribute to the negative axial springs. The capacitance, excitation frequency, and voltage of the LCR circuits, and the negative stiffness were among the variable parameters in the simulation study.

A typical stable transient behavior is shown in Figures 4 and 5. Figure 4 shows the impeller settles 0.106 below the reference position (Z=0) that is 0.381 mm below the bearing stator. In other words, the gap between the impeller and the bearing stator is 0.487 mm. Figure 4 also shows the amplitudes of the three LCR currents are all about 0.5-ampere peak to peak.

Figure 5 shows the impeller angles θ_x and θ_y stabilize to zero from arbitrary initial conditions of ±1 milliradian. The results of these two figures indicate the stability of the system for the desired design parameters.

The parametric study observed that steady-state tilt angles (θ_x, θ_y) were possible due to uneven strength of the channels, which may be due to capacitor tolerance and/or uneven excitation voltage, and so forth. For the strength of a channel, we mean the force it produces. Note that the force is proportional to the current squared. Therefore, the force is an average of the ac force at doubled the excitation frequency.

PUMP FABRICATION AND TEST

Development of the pump occurred in two phases: proof of feasibility in Phase I and demonstration of an implantable pump prototype in Phase II. Using the Phase I pump as the starting point, the Phase II design effort reduced the impeller diameter from 51 to 38 mm, a 25% reduction. The first Phase II pump fabricated was a rapid prototype made of stereolithography (SLA)/epoxy components. The final pump prototype was made of titanium.

Levitation tests were performed on the rapid prototype pump. The pump was submerged in a water bath, which was then placed on top of a hollow tube. A high-intensity fiber-optic light source was fed up through the tube and used to illuminate the assembly.

Successful levitation was confirmed visually and the requisite magnetic gap observed. Figure 6 shows the pump's pressure versus flow characteristics, which were close to analytical predictions.

Two titanium pump prototypes were put on a test loop (Figure 7) and tested for performance. The pumps successfully demonstrated operation at the design condition of 5 liter/min, 100 mmHg.

Figure 8 presents a comparison of current waveforms of the LCR circuits from the rapid prototype and the final pump. Figure 8 indicates the instability (impeller wobble) present in the rapid prototype, while the high-frequency waveforms from the final pump (Figure 9) are not significantly modulated by low-frequency mechanical vibration due to impeller instability. The average current amplitudes of the three phases shown in Figure 9 are of equivalent size, indicating that all three LCR circuits are carrying equal load to keep the magnetic gap consistent.

One titanium pump was placed on endurance test in June 2007 and has since operated without incident at the design point (5 liter/min, 100 mmHg). Pump casing vibration levels over the course of endurance testing have also been observed to be low, varying from 0.002 to 0.025 g-rms (see Figure 10). Temperatures of the motor and LCR coils are below 38°C, indicating good thermal management in the pump design.

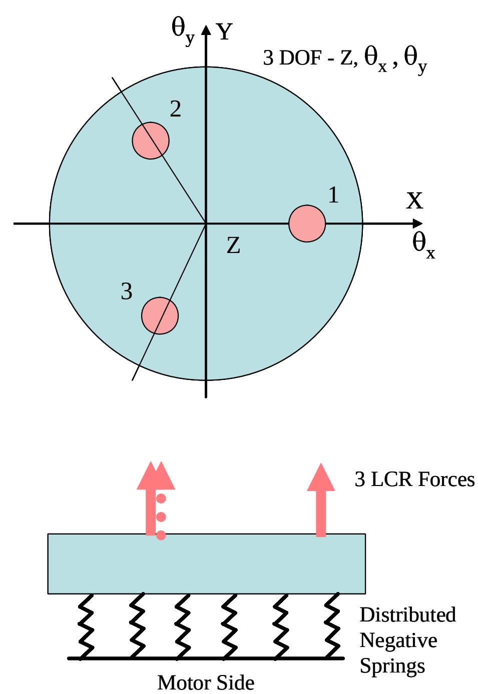

FIGURE 3: Mathematical model used to assess dynamic rotor stability

TABLE 1: System equations of motion

```
dy(1) = y(2) ;
dy(2) = -R1/L1*y(2) -1/(L1*C1)*y(1)+
Eo1/L1*sin(2*pi*Hz*t) ;
dy(3) = y(4) ;
dy(4) = -R2/L2*y(4) -1/(L2*C2)*y(3)+
Eo2/L2*sin(2*pi*Hz*t) ;
dy(5) = y(6) ;
dy(6) = -R3/L3*y(6) -1/(L3*C3)*y(5)+
Eo3/L3*sin(2*pi*Hz*t) ;

dy(7) = y(8) ;
dy(8) = (-D*y(8)+Pull-Km*y(7) + FM1+FM2+FM3)/Mass;
dy(9) = y(10) ;
dy(10) = (-Dth*y(10)-Kth*y(9) + 0.866*Rpole*FM2 -
0.866*Rpole*FM3+H*y(12))/It;
dy(11) = y(12) ;
dy(12) = (-Dth*y(12)-Kth*y(11)-
Rpole*FM1+0.5*Rpole*FM2+0.5*Rpole*FM3 -
H*y(10))/It;
```

Notes
"d" implies derivative with respect to time.
D, Dth = linear and angular damping coefficient, respectively, due to liquid squeeze film.
R1, R2, R3 = resistance
L1, L2, L3 = inductance
C1, C2, C3=capacitance
Eo1, Eo2, Eo3 = amplitude of excitation voltage
Hz = excitation frequency
Y(2),Y(4), Y(6) = LCR currents
Y(7),Y(9),Y(11) = Z, θx, θy
H = angular momentum
Rpole = force center radius of pole
Km, Kth = linear, angular stiffness of motor and radial PM bearing.

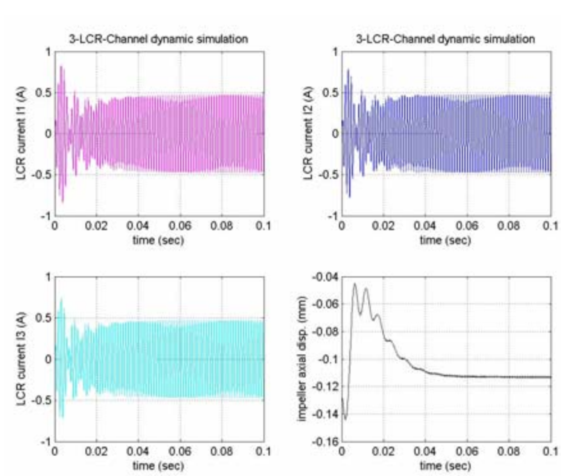

FIGURE 4: Simulated stable transient behavior of impeller and LCR current amplitudes

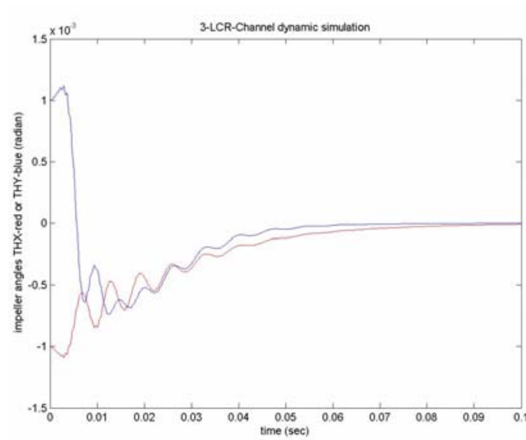

FIGURE 5: Pump stability as indicated by impeller angles

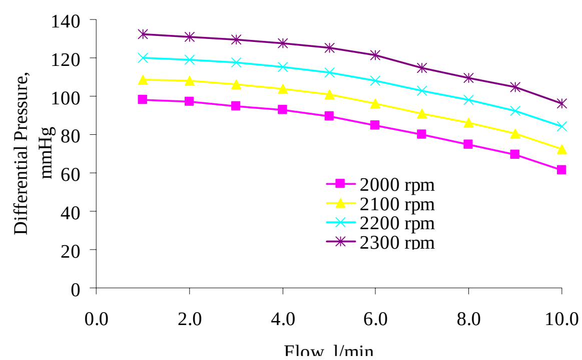

FIGURE 6: Demonstrated pump pressure versus flow characteristics are close to analytical predictions

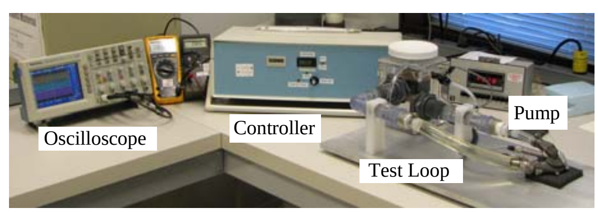

FIGURE 7: Pump endurance test setup

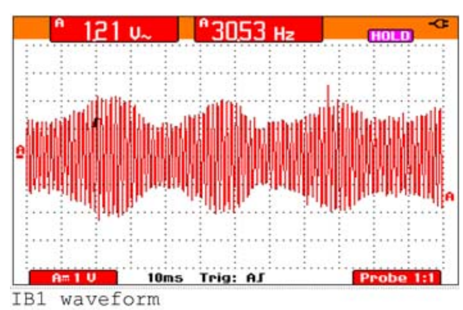

FIGURE 8: Significant modulation in current waveforms of rapid prototype pump

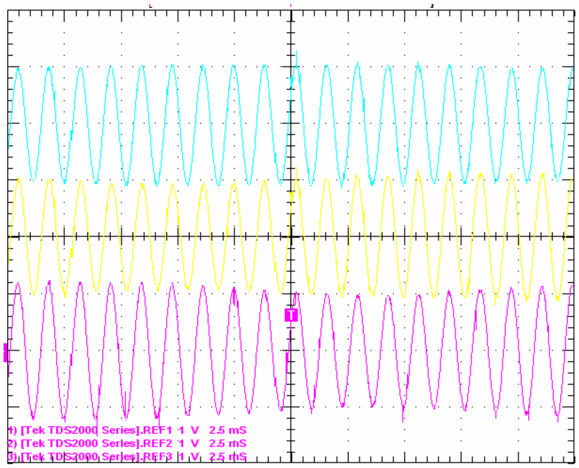

FIGURE 9: Three current waveforms from titanium pump show minimal modulation

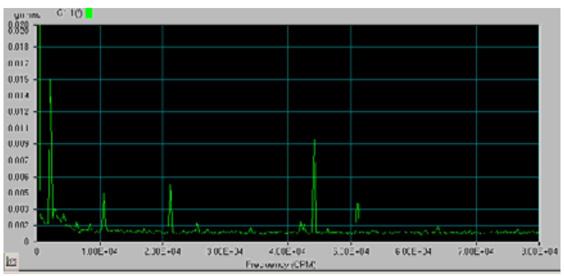

FIGURE 10: Casing vibration levels of pump on endurance test (vibration at 2,000-rpm running speed = 0.015 g rms)

SUMMARY AND CONCLUSIONS

A compact centrifugal blood pump suitable for use as an implantable LVAD has been developed. On one side of the pump is an axial gap motor; on the other is a bearing stator, which consists of three sensorless LCR bearings in the axial direction, and a PM ring bearing for the radial direction. The impeller is 38 mm in diameter and totally magnetically levitated, taking advantage of liquid damping from the squeeze film between the impeller and bearing stator.

Although the pump structure is simple, the static and dynamic interactions among the magnetic elements (impeller, bearings, and motor) are complex. To facilitate the design process, the relationships among forces and stiffness of the magnetic elements were carefully formulated.

Based on this design methodology, two titanium pumps were built and tested. These pumps delivered flow of 5 liter/min at a pressure of 100 mmHg with a power consumption of approximately 5 W. Two pumps remain on endurance test and have accumulated more than 13,000 hr, demonstrating low temperatures in the motor and bearing stators, along with low casing vibration.

REFERENCES

1. Jin, J. and T. Higuchi, “Dynamics and Stabilization of Magnetic Suspension using Tuned LC Circuit,” Proceedings, 4th International Symposium on Magnetic Bearings, August 1994, Zurich, p. 321-326.
2. Wurmsdobler, P., “Stable magnetic suspension in fluids using tuned LC-circuits,” Proceedings, 7th International Symposium on Magnetic Bearings, August 2000, Zurich.
3. Chen, H. Ming, et al., “Development of Magnetically Levitated Blood Pumps,” Presented at 6th International Symposium on Magnetic Suspension Technology, Turin, Italy, October 7-11, 2001.
4. Chen, H. Ming and T. Walter, “A Foil-Magnetic Thrust Bearing Using LCR Circuit,” 10th International Symposium on Magnetic Bearings, Martigny, Switzerland, August 21-23, 2006.
5. Jin, J. and T. Higuchi, “Current Feedback Stabilization of Tuned Magnetic Suspension System,” Proceedings, 5th International Symposium on Magnetic Bearings, Kanazawa, Japan, August 1996.
6. Chen, H. Ming, et al., “Rotary Pump with Electromagnetic LCR Bearing,” International Patent Application WO 2005/034312 A2, April 14, 2005.